

Osteoarthritis and Cartilage (2009) 17, 73–82

© 2008 Published by Elsevier Ltd on behalf of Osteoarthritis Research Society International.

doi:10.1016/j.joca.2008.05.019

Osteoarthritis and Cartilage

**International
Cartilage
Repair
Society**

Analysis of radial variations in material properties and matrix composition of chondrocyte-seeded agarose hydrogel constructs

T.-A. N. Kelly Ph.D.†, K. W. Ng Ph.D.†, G. A. Ateshian Ph.D.‡ and C. T. Hung Ph.D.†*

† *Cellular Engineering Laboratory, Department of Biomedical Engineering, Columbia University, New York, NY 10027, USA*‡ *Musculoskeletal Biomechanics Laboratory, Department of Mechanical Engineering, Columbia University, New York, NY 10027, USA*

Summary

Objective: To examine the radial variations in engineered cartilage that may result due to radial fluid flow during dynamic compressive loading. This was done by evaluating the annuli and the central cores of the constructs separately.

Method: Chondrocyte-seeded agarose hydrogels were grown in free-swelling and dynamic, unconfined loading cultures for 42 days. After mechanical testing, constructs were allowed to recover for 1–2 h, the central 3 mm cores removed, and the cores and annuli were retested separately. Histological and/or biochemical analyses for DNA, glycosaminoglycan (GAG), collagen, type I collagen, type II collagen, and elastin were performed. Multiple regression analysis was used to determine the correlation between the biochemical and material properties of the constructs.

Results: The cores and annuli of chondrocyte-seeded constructs did not exhibit significant differences in material properties and GAG content. Annuli possessed greater DNA and collagen content over time in culture than cores. Dynamic loading enhanced the material properties and GAG content of cores, annuli, and whole constructs relative to free-swelling controls, but it did not alter the radial variations compared to free-swelling culture.

Conclusion: Surprisingly, the benefits of dynamic loading on tissue properties extended through the entire construct and did not result in radial variations as measured *via* the coring technique in this study. Nutrient transport limitations and the formation of a fibrous capsule on the periphery may explain the differences in DNA and collagen between cores and annuli. No differences in GAG distribution may be due to sufficient chemical signals and building blocks for GAG synthesis throughout the constructs.

© 2008 Published by Elsevier Ltd on behalf of Osteoarthritis Research Society International.

Key words: Type I collagen, Type II collagen, Elastin, Glycosaminoglycans, Correlation analysis, Mechanical properties.

Introduction

Functional tissue engineering of articular cartilage aims to engineer samples whose mechanical properties mimic those of the native tissue. Since the primary mode of loading of articular joints under physiological conditions is dynamic compression, we adopted a dynamic deformational loading bioreactor system^{1,2}. In unconfined compression, samples are loaded between impermeable, smooth platens and are free to expand laterally (radially/circumferentially), thereby produces both compressive (axially) and tensile (radially/circumferentially) strains, which better represents the physiologic loading environment as suggested by analyses of contacting cartilage layers^{3,4}. This loading configuration produces more uniform mechanical signals throughout the cylindrical samples than confined compression with a porous platen, which produces compaction at the tissue–platen interface. Additionally, the uniformity of

the compression-induced interstitial fluid pressure through the sample depth is also more physiologic⁴.

In this study, we follow-up on our previous analysis of construct inhomogeneity through the thickness², by investigating the material development in the radial direction. In addition to subjecting constructs to radial tensile strains, unconfined compression loading generates a pressure gradient where the fluid pressurization is highest in the central region and lowest at the radial edge, resulting in maximal fluid flow at the radial edge^{5–8}. Several investigators have reported that dynamic loading of cartilage explants in unconfined compression preferentially stimulates chondrocyte biosynthetic activity at the periphery of cylindrical samples and have attributed this spatially dependent biosynthesis to the higher fluid flow levels at the construct edge^{9–11}. The influence of these radially dependent stimuli, established by the unconfined compression loading configuration, on development of engineered cartilage constructs has not been investigated.

Here, we sought to determine if applied dynamic loading (3 h/day, free-swelling 21 h/day) can alter the radial inhomogeneity of constructs vs free-swelling controls (24 h/day). We hypothesized that the radial inhomogeneity will be enhanced in loaded samples vs free-swelling controls, due to the loading-enhanced fluid flow stimulation at the

*Address correspondence and reprint requests to: Dr Clark T. Hung, Ph.D., Department of Biomedical Engineering, Columbia University, 351 Engineering Terrace, 1210 Amsterdam Avenue, MC 8904, New York, NY 10027, USA. Tel: 1-212-854-6542; Fax: 1-212-854-8725; E-mail: cth6@columbia.edu

Received 5 April 2007; revision accepted 23 May 2008.

periphery. Our microscopy-based technique, previously used for investigating the inhomogeneity through the construct thickness, is limited to samples of thickness much less than that of the radius of our constructs; consequently, an alternative testing methodology was developed for the current study². Constructs cultured for 6 weeks under free-swelling or dynamic loading were mechanically tested whole as well as after concentric coring, to permit study of both the outer annulus and the 3-mm central core region on days 0, 14, 28, and 42. Complementary biochemical and histological analyses were conducted for the cores and annuli to permit study of the radial inhomogeneity of these parameters.

Materials and methods

Primary chondrocytes were harvested from the carpometacarpal joints of 3–4 months old calves *via* digestion in Dulbecco's Modified Eagle's Medium (DMEM, Mediatech, Herndon, VA) containing 5% fetal bovine serum (FBS, Atlanta Biochemical, Atlanta, GA) and 390 U/ml collagenase (Sigma, St. Louis, MO). Cells were encapsulated in 2% type VII agarose (Sigma) at 60×10^6 cells/ml and equilibrated for 3 days in DMEM containing 5%FBS. After this 3-day period (study day 0), disks ($\varnothing 5.0 \times 2.3$ mm) were cored and cultured in 100 mm Petri dishes (20–25 disks/plate) with 30 ml of DMEM supplemented with buffers, antibiotics, antimycotics, amino acids, 20%FBS and 50 μ g/ml ascorbic acid (Sigma), with daily media change.

The constructs were either dynamically loaded, as described previously², or maintained under free-swelling conditions through a 6-week culture period. Briefly, a custom loading device was utilized to impose a continuous sinusoidal deformation (2% tare strain, 10% peak-to-peak strain, 1 Hz) for 3 h/day, 5 days/week. Agarose templates with 8 mm diameter wells were utilized to ensure that the constructs were properly seated and prevent shifting during dynamic unconfined compression loading or transport. Prior to loading, the disks were transferred to the molds and loaded in 5 ml of media. Free-swelling controls were transferred and maintained adjacent to the device during the loading. After loading, the disks were returned to the 100 mm dishes, randomly flipped to reduce any orientation bias, and maintained as described above.

At days 0, 14, 28, and 42, a custom unconfined compression device, with rigid-impermeable glass loading platens, was used to measure the equilibrium and dynamic compressive moduli of the constructs¹². Before each test, the disk thickness and diameter were measured, and the specimens were equilibrated in creep, under a tare load of 0.01 N. A stress-relaxation test was then performed, with a ramp speed of 1 μ m/s until the displacement reached 10% of the post-tare load thickness. Constructs were allowed to equilibrate for 20 min. The equilibrium modulus was calculated from the equilibrium reaction force, the sample's cross-sectional area, and the applied strain. Following stress-relaxation test, a sinusoidal displacement of 2% strain was applied at 0.5 Hz and the dynamic modulus was calculated from the load and displacement profiles, and the construct geometry. Each construct was tested whole, as described above, and then allowed to recover for 1–2 h prior to coring with a 3 mm dermal punch mounted on a custom cutting rig, which was used to align and stabilize the constructs during coring. The annuli and central 3 mm cores were then tested separately. For half the samples, the annuli were tested first and for the other half the cores were tested first. Images of typical constructs, before and after coring, are presented in Fig. 1. After mechanically testing, the disks were fixed in 3.7% formaldehyde, 5% acetic acid, 70% ethanol¹⁸ for histology or stored at -30°C for biochemistry.

The samples for biochemical analyses were thawed, weighed wet, lyophilized, weighed dry, and digested for 16 h at 60°C in proteinase K in 50 mM tris buffered saline containing 1 mM ethylenediaminetetraacetic acid, 1 mM iodoacetamide and 10 μ g/ml pepstatin A¹³. The DNA content was quantified using the PicoGreen assay (Invitrogen, Carlsbad, CA)¹⁴, using lambda phage DNA (0–1 μ g/ml) as a standard. The glycosaminoglycan (GAG) content was measured using the 1,9 dimethylmethylene blue (Sigma) dye-binding assay¹⁵, using shark chondroitin sulfate (0–50 μ g/ml) as a standard. The collagen content was measured using the orthohydroxyproline (OHP) colorimetric assay¹⁶, using bovine OHP (0–10 μ g/ml) as a standard. Here, the digests were hydrolyzed in equal volume of 12 M HCl at 110°C for 18 h, dried in the presence of sodium hydroxide, and resuspended in 1 ml of solution prior to analysis. Collagen content was calculated using a 1:10 OHP-to-collagen mass ratio¹⁷.

Histology samples were dehydrated, paraffin-embedded, sectioned (8 μ m), and mounted onto microscope slides. Prior to labeling, samples were dewaxed and rehydrated. GAG and collagen were stained with Safranin O (Sigma) and Picrosirius Red (Sigma), respectively. Immunohistochemistry samples were digested in 0.5 mg/ml testicular hyaluronidase (Sigma), swollen in 0.5M acetic acid, blocked in 10% normal goat serum (NGS),

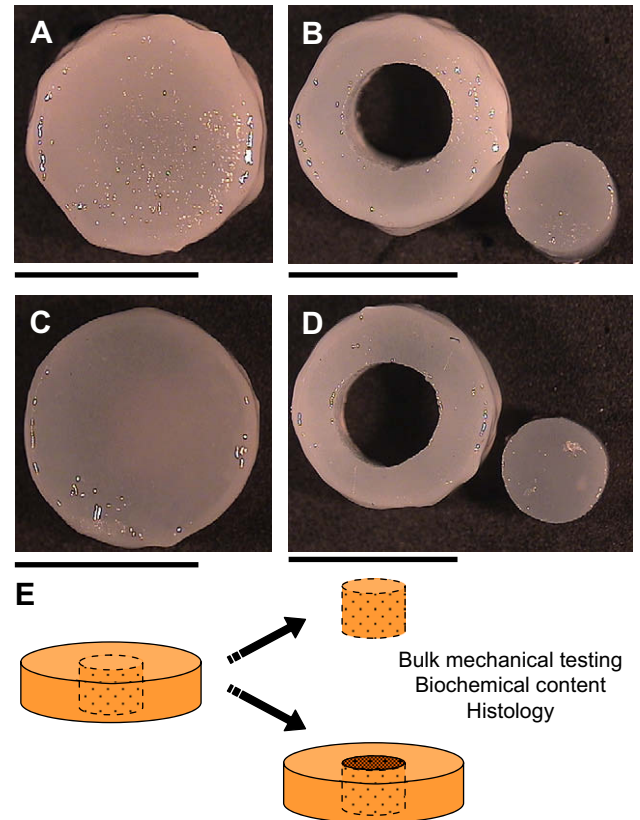


Fig. 1. Images of free-swelling (A, B) and dynamically loaded (C, D) constructs were acquired at day 42, before (A, C) and after (B, D) coring of the constructs. Scale bars equal 5 mm. For this study, samples were tested whole, allowed to recover and then the annuli and cores were tested separately (E).

and immuno-labeled in 10%NGS containing monoclonal antibody against collagen I (MAB3391, Chemicon, Temecula, CA), collagen II (II-I16B3, Developmental Studies Hybridoma Bank, Iowa City, IA), and elastin (BA-4, Sigma). Non-immune controls were incubated in 10%NGS. Samples were then incubated in Alexa Fluor 488 goat anti-mouse secondary antibody (Invitrogen) and propidium iodide (Invitrogen), then analyzed with an Olympus Fluoview confocal system (NY/NJ Scientific, Middlebush, NJ) *via* dual wavelength excitation at 488 and 568 nm ($20\times$).

Statistica (Statsoft, Tulsa, OK) was used to perform statistical analysis using multivariate analysis of variables ANOVA, with sample geometry, time, and loading condition as the independent variables. If significant trends were observed with ANOVA, Tukey *post hoc* test was used to determine significant inter-group differences. $P < 0.05$ was considered significant. Four samples were tested per group and are presented as mean \pm standard deviation. Statistica was also used to determine the Pearson product moment correlation coefficient and significant differences ($P < 0.05$) between the biochemical composition and the material properties of the constructs.

Results

Changes in wet and dry weights, water content, and biochemical composition of the intact chondrocyte-seeded constructs are presented in Fig. 2. The values and trends observed for these samples were similar to those previously reported by our group^{1,2}. Here, significant effects of time was observed for all measures except for the DNA content when normalized to the wet weight ($P < 0.005$), however, there were no significant effects of loading. The wet weight and overall DNA content doubled over the 6-week culture period, whereas the dry weight exhibited a four-fold increase. When normalized to the wet weight, the DNA

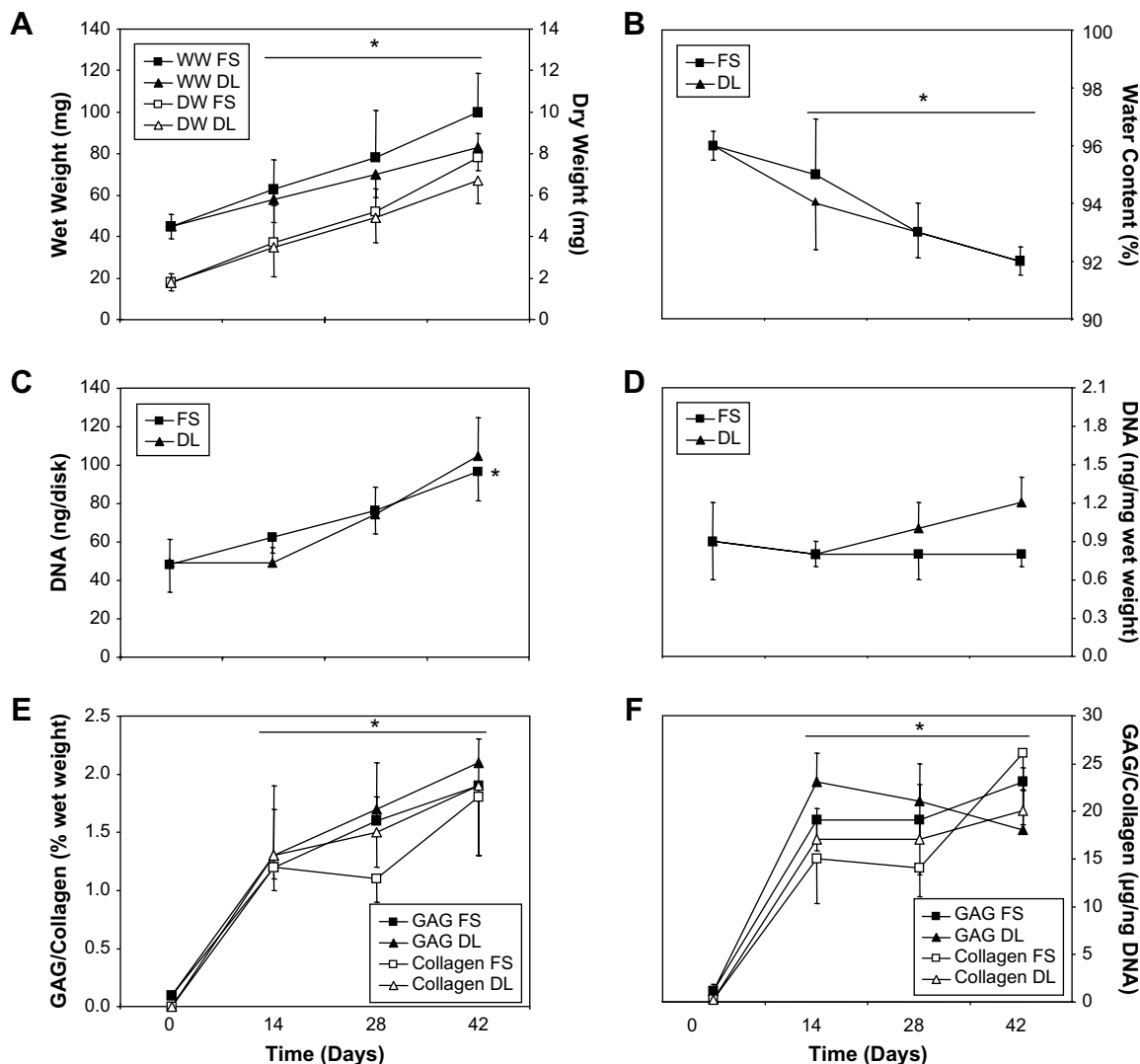


Fig. 2. Wet and dry weights (A), water content (B), DNA content (C, D), and GAG and collagen contents (E, F) of intact, free-swelling and dynamically loaded chondrocyte-seeded constructs. *Represents significant differences vs day 0 constructs (ANOVA $P < 0.005$; *post hoc* $P < 0.005$).

content of the free-swelling constructs remained constant through the 6-week culture period, however, dynamically loaded constructs exhibited a 33% increase that was not statistically significant.

The wet and dry weights [Fig. 3(A and B), respectively] of the annuli and cores were similar at day 0. Over time, these variables remained constant for 3 mm cores, however, there was a significant temporal increase in the weights of the annuli by day 28 ($P < 0.0005$) that parallel the trends observed for the whole constructs [compare Fig. 2(A) to Fig. 3(A and B)]. Additionally, the wet and dry weights of the annuli were significantly greater than the cores by day 14 for the wet weight ($P < 0.005$) and day 28 for the dry weight ($P < 0.0005$). There was a significant effect of load in the annuli at day 42 ($P < 0.05$). There was a resultant significant temporal decrease in the water content [Fig. 3(C)] of the both the annuli and cores of the constructs ($P < 0.005$), however, there were no significant inter-group differences.

The temporal changes in the DNA content [Fig. 3(D)] was similar to those observed for the wet and dry weights. Here,

the absolute DNA content of the cores was 36% lower than the annuli on day 0 [Fig. 3(D)], though no difference was found in the wet weight-normalized DNA content [Fig. 3(E)]. There was a three-fold increase in the absolute DNA content of the annuli, and 37% and 21% decrease in the absolute DNA content of the cores of the free-swelling and dynamic loading constructs, respectively, over time in culture. This decrease in the cores, however, was not statistically significant. There was a significant effect of time in the annuli of the constructs by day 28 ($P < 0.05$). Additionally, the DNA content of the annuli was significantly greater than the cores by day 28 for the dynamically loaded constructs and by day 14 for the free-swelling controls ($P < 0.01$). When normalized to the wet weight, the DNA content [Fig. 3(E)] of the free-swelling annuli and dynamically loaded cores showed a 10% reduction over the 6-week culture period, however, there were no significant temporal changes. Here, the DNA content of the annuli was significantly greater than the cores by day 28 in the free-swelling constructs and by day 42 in the dynamically loaded constructs ($P < 0.05$).

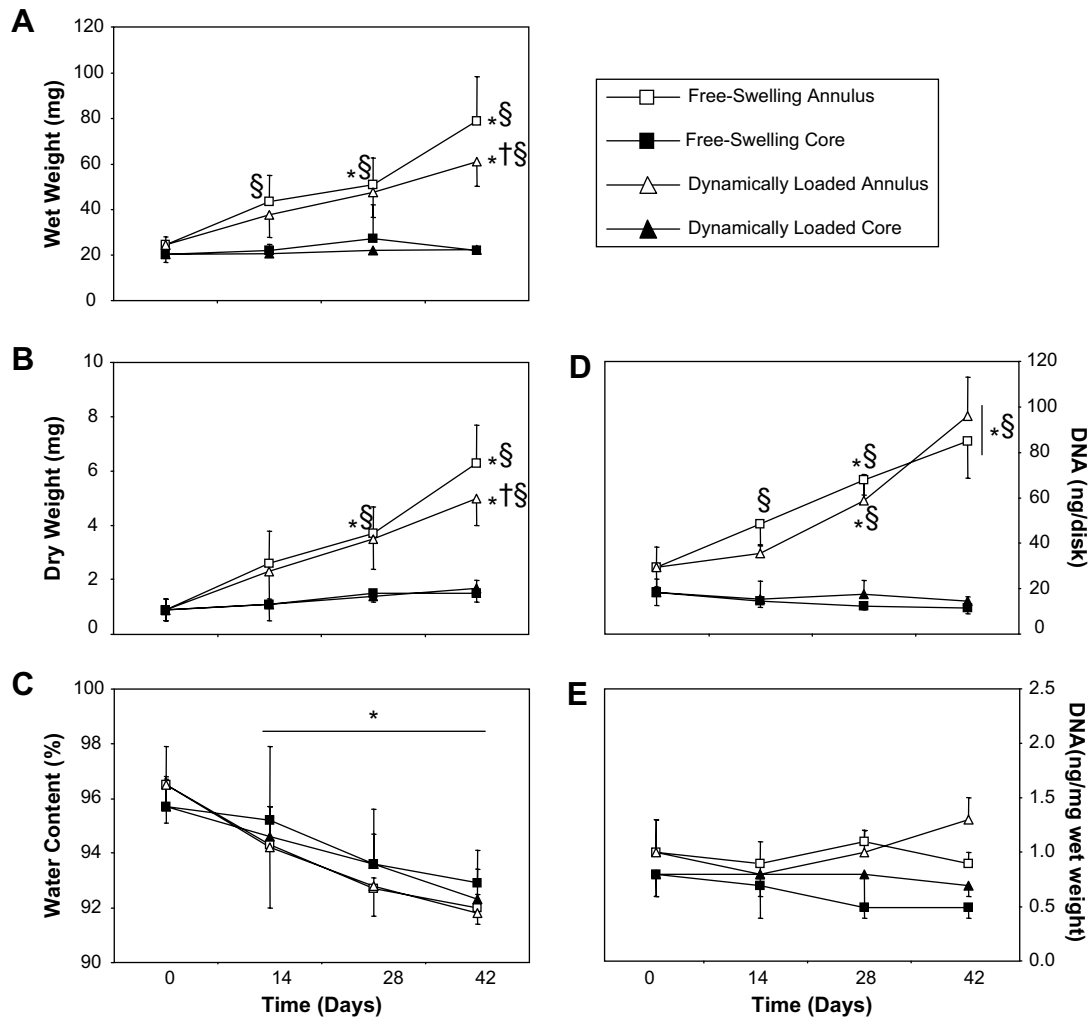


Fig. 3. Wet weight (A), dry weight (B), water content (C), and DNA content (D, E), of the annuli (open) and cores (closed) of free-swelling (boxes) and dynamically loaded (triangles) constructs over the 6-week culture period ($n = 4-9$). Significant effect of time was observed for these samples (ANOVA $P < 0.05$). *Represents significant differences vs day 0 constructs (ANOVA $P < 0.05$; *post hoc* $P < 0.05$); †represents significant differences vs free-swelling controls (ANOVA $P < 0.01$; *post hoc* $P < 0.05$); §represents significant differences vs the respective cores (ANOVA $P < 0.001$; *post hoc* $P < 0.05$).

The GAG and collagen contents of these constructs increased over time for all groups (Fig. 4), with significant changes occurring by day 14 ($P < 0.05$). Significant differences in the GAG content with loading were observed at day 42 in the annuli and cores when the data was normalized to the wet weight ($P < 0.05$), but only in the cores when data was normalized to the DNA content ($P < 0.05$). Additionally, the annuli and cores were significantly different for the day 42 free-swelling constructs when the GAG content was normalized to the wet weight ($P < 0.05$). By day 28, the GAG/DNA value was significantly greater in the cores than in the annuli ($P < 0.05$). By day 14, the collagen content of the annuli of both free-swelling and dynamically loaded constructs was significantly greater than the corresponding cores ($P < 0.05$). Additionally, the collagen/DNA value of the day 42 dynamically loaded cores was significantly greater than the correspondent annuli and free-swelling samples ($P < 0.01$).

The mechanical properties of all groups increased significantly over time in culture (Fig. 5; $P < 0.008$). There was a significant effect of loading on the equilibrium modulus

by day 42 [Fig. 5(A); $P < 0.005$]. A significant decrease in equilibrium modulus [Fig. 5(A)] was observed for the dynamically loaded cores at day 14 ($P < 0.004$). Additionally, there was a significant effect of loading on the dynamic modulus by day 28 for the whole constructs and the annuli and by day 42 for the cores [Fig. 5(B-D); $P < 0.005$]. Similar results were obtained at other loading frequencies (data not shown). As the dynamic modulus is a structural property with fluid flow dependence^{12,19}, this parameter would be affected by the differences in the geometry and boundary conditions between the cores, annuli, and whole disks. Therefore, comparisons between the three geometric configurations were not performed.

Correlation analysis of the relationship between GAG and collagen content and the moduli of chondrocyte-seeded constructs are presented in Table I. For the free-swelling constructs, there were no observed correlation between the material properties and the biochemical content. For the intact dynamically loaded constructs, significant positive correlation was observed between the GAG content and the equilibrium modulus and dynamic modulus, and between

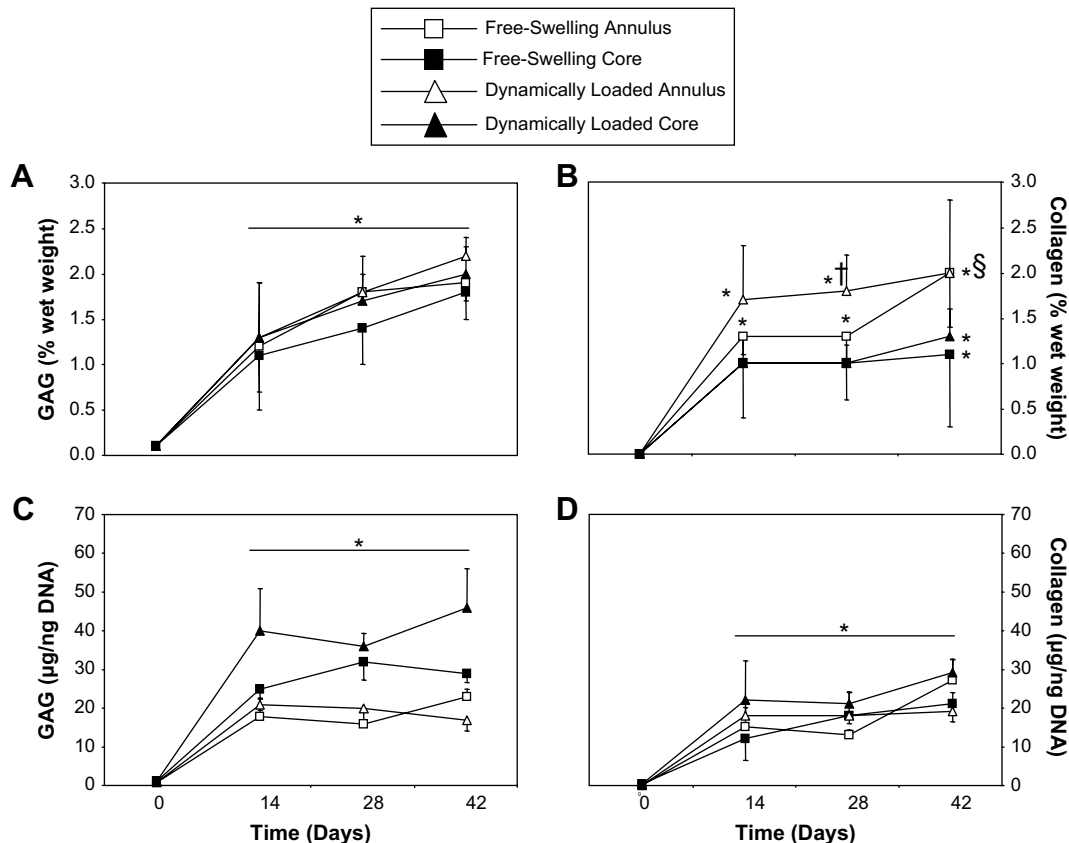


Fig. 4. GAG (A, B) and collagen (C, D) contents of the annuli (open) and cores (closed) of free-swelling (boxes) and dynamically loaded (triangles) constructs over the 6-week culture period ($n=4-9$). Significant effect of time was observed for these samples (ANOVA $P < 0.05$). *Represents significant differences vs day 0 constructs (ANOVA $P < 0.05$; *post hoc* $P < 0.05$); †represents significant differences vs free-swelling controls (ANOVA $P < 0.05$; *post hoc* $P < 0.05$); ‡represents significant differences vs the respective cores (ANOVA $P < 0.05$; *post hoc* $P < 0.05$).

the collagen content and the dynamic modulus. These correlations were lost in the annuli, but were maintained in the cores. Additionally, a significant positive correlation was observed between the collagen content and the equilibrium modulus for the dynamically loaded cores.

Safranin O and Picrosirius Red staining (Fig. 6) were intense in the center of both free-swelling [Fig. 6(B and H)] and dynamically loaded [Fig. 6(E and K)] constructs at day 42. Along the circumferential [Fig. 6(A,D,G,J)] and axial [Fig. 6(C,F,I,L)] surfaces, all constructs possessed a dense GAG and collagen-rich layer. Along the axial surface, this layer was thinner, more intensely stained, and smoother in the dynamically loaded construct [Fig. 6(F and L)] than in the free-swelling control [Fig. 6(C and I)].

At day 42, the type II collagen staining [Fig. 7(A–F)] was intense for both free-swelling and dynamically loaded constructs along the axial and radial edges [Fig. 7(A,C,D,F)] than in the central region [Fig. 7(B and E)]. There was a cell-dense type II collagen-free region around the periphery of both groups [Fig. 7(A,C,D,F)]. Along the axial edge [Fig. 7(C and F)], this region was more extensive in the free-swelling construct [Fig. 7(C)] than for the dynamically loaded construct [Fig. 7(F)]. Additionally, staining in the center was more intense for the dynamically loaded construct [Fig. 7(E)] than the free-swelling construct [Fig. 7(B)].

At day 42, type I collagen [Fig. 7(G–L)] and elastin [Fig. 7(M–R)] immunofluorescence showed that the fibrous

outer layer is composed primarily of type I collagen in the free-swelling constructs and elastin in the dynamically loaded constructs [compare Fig. 7(G,I,J,L) to Fig. 7(M,O,P,R)]. Interestingly, for the dynamically loaded constructs, type I collagen staining was more intense on the radial (unloaded) edge than on the axial (loaded) edge [Fig. 7(J and L)]. In the central region of the constructs, a small amount of type I collagen [Fig. 7(H and K)] and elastin [Fig. 7(N and Q)] staining were observed for both free-swelling and dynamically loaded constructs. Type I collagen labeling was more intense in the central region of the dynamically loaded constructs [Fig. 7(K)] compared to free-swelling controls [Fig. 7(H)], however, similar levels of elastin staining was observed in the central region of both groups of constructs [Fig. 7(N and Q)].

Discussion

The results of this study represent the first published attempt known to the authors that seeks to characterize the development of engineered cartilage tissue in the radial direction. Consistent with our previous findings^{2,20–22}, the moduli of the dynamically loaded constructs in the presented study were generally greater than free-swelling counterparts (for whole constructs as well as respective central core and annuli regions). Interestingly, the relative

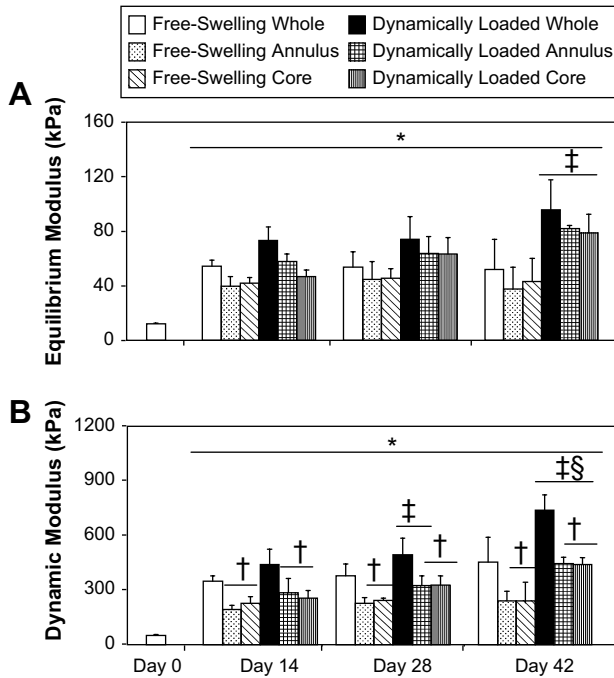


Fig. 5. Equilibrium (A) and dynamic (B; measured at 0.5 Hz) moduli of free-swelling and dynamically loaded constructs over the 42-day culture period ($n = 7$). The constructs were allowed to recover for 1 h before the annulus and the 3 mm central core were tested. As the dynamic modulus is a structural property, inter-group comparisons between intact constructs (B), annuli (C), and cores (D) were not performed. *Represents significant differences compared to day 0 (ANOVA $P < 0.005$; Tukey $P < 0.003$); †represents significant differences compared to corresponding free-swelling controls (ANOVA $P < 0.0005$; Tukey $P < 0.005$); ‡represents significant differences compared to whole sample (ANOVA $P < 0.0005$; Tukey $P < 0.02$); §represents significant differences compared to day 28 constructs ($P < 0.05$).

radial variation in material properties was unaffected by loading, with inner and peripheral regions derived from the constructs having similar equilibrium modulus and GAG content, with both cores and annuli possessing an improved equilibrium modulus under dynamic loading. This is a surprising result given that it was expected that the radial fluid flow arising during unconfined cyclical compression would preferentially affect the region of the construct encompassed by the annulus^{9–11} and not be transmitted through

to the center of the construct. We, therefore, must reject our hypothesis that dynamically loaded constructs exhibit different radial inhomogeneity than free-swelling constructs. In this regard, our findings for radial distribution in properties are reminiscent of those previously reported for axial distribution in properties, where the profile of the relative depth-varying modulus is similar for free-swelling and loaded constructs².

Coring of the constructs appeared to significantly reduce the dynamic modulus of both the cores and annuli compared to the respective intact samples [Fig. 5 (B–D)]. However, given that the dynamic modulus depends on the fluid pressurization within the sample^{12,19}, this apparent reduction may be due to changes in the fluid flow boundary conditions resulting from the coring technique. Therefore, inter-group comparisons between the dynamic moduli of cores, annuli, and whole constructs were avoided. The lack of significant differences in the equilibrium modulus between the cores and annuli, however, remains valid given that this measurement is a material property that is normalized to geometry and determined at equilibrium, thereby being fluid flow independent. The effects of dynamic loading also appear to be genuine as dynamic loading increased the measured mechanical properties regardless of sample geometry.

Histological analysis reveals the presence of a thick cell-rich fibrous layer that encompasses the entire construct in either culture condition, though dynamic loading lessened the presence of this layer along the loaded surfaces, as previously reported^{22–24}. The formation of this fibrous layer has been linked to fetal bovine serum²⁴ and may be due to the proliferation of cells that have crawled out (or been pushed out) onto their outer surfaces of the constructs. Immunostaining for type I and II collagen and elastin showed that the cell-rich fibrous layer is devoid of type II collagen²⁵. However, the free-swelling and dynamically loaded constructs showed disparate type I collagen and elastin staining, with free-swelling constructs primarily expressing type I collagen and dynamically loaded constructs primarily expressing elastin at their peripheries. Dynamic loading appeared to downregulate the production of type I collagen while upregulating the production of elastin on the loaded surface, thereby reducing the differentiation of cells along the surface of the tissue. This downregulation of type I collagen production with loading has been reported in the literature²⁵. These results are encouraging because elastin has been shown to be expressed in the superficial zone of cartilage^{26,27} and may represent an adaptation of the articular surface *in vivo* due to mechanical stresses. This fibrous

Table I

Pearson's product moment correlation coefficient (R) of the biochemical and material properties of the chondrocyte-seeded agarose constructs. Pearson's correlation results relating biochemical constituents (GAG and collagen; normalized to the wet weight) to mechanical properties compressive and dynamic moduli of annuli and cores free-swelling (FS) and dynamically loaded (DL) constructs. Significant P values are bolded ($n = 4–5$)

Loading		Pearson's R (P)		
		Whole	Annulus	Core
FS	GAG vs equilibrium modulus	−0.11 (0.737)	0.42 (0.139)	0.25 (0.438)
	Collagen vs equilibrium modulus	0.12 (0.731)	0.16 (0.667)	0.07 (0.833)
	GAG vs dynamic modulus	0.42 (0.228)	0.40 (0.157)	0.25 (0.429)
	Collagen vs dynamic modulus	0.47 (0.175)	0.59 (0.072)	0.18 (0.566)
DL	GAG vs equilibrium modulus	0.71 (0.007)	0.42 (0.139)	0.56 (0.048)
	Collagen vs equilibrium modulus	0.38 (0.353)	0.12 (0.695)	0.62 (0.023)
	GAG vs dynamic modulus	0.70 (0.007)	0.40 (0.157)	0.69 (0.009)
	Collagen vs dynamic modulus	0.69 (0.009)	0.05 (0.852)	0.65 (0.016)

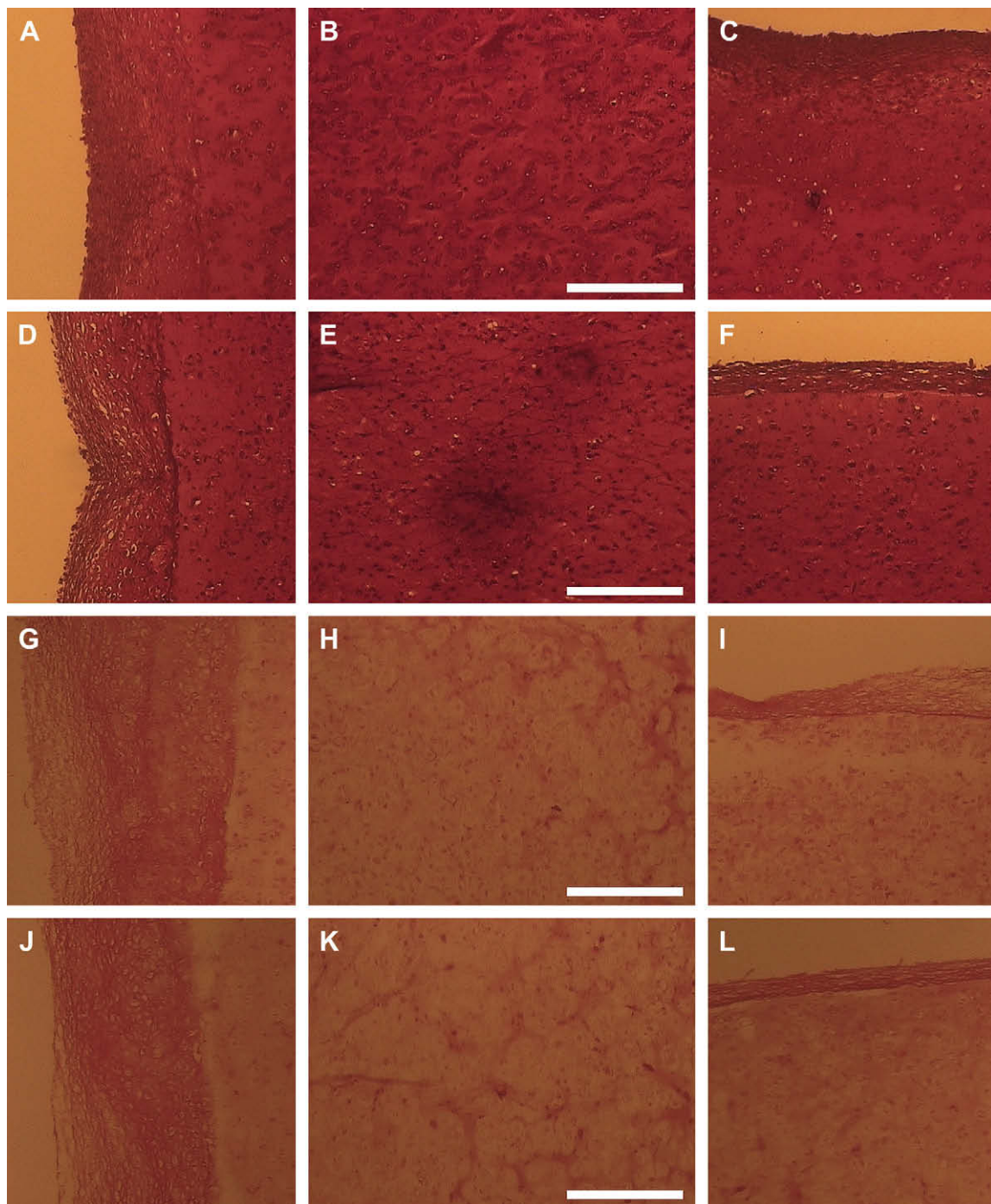


Fig. 6. Safranin O (GAG; A–F) and Picrosirius Red staining (collagen; G–L) of free-swelling (A–C, G–I) and dynamically loaded (D–F, J–L) constructs on day 42. Images were acquired along the radial edge (first column), in the center (second column), and along the axial edge (third column) of the constructs. Scale bars equal 250 μ m.

layer has been found to affect the mechanical properties of cartilage explants²⁸ and, therefore, may also have had an unmeasured effect on the mechanical properties of the engineered cartilage in this study, particularly the annuli. The compromising of this layer due to coring may also have some effect on the measured decrease in mechanical properties of cores and annuli when compared to intact samples.

Positive correlations were found between the GAG content and the moduli of constructs, and between the collagen content and the dynamic moduli of the intact constructs, consistent with previous publications from our laboratory²¹. However, these correlations were not strong or consistent among all groups, nor did they necessarily persist after coring of the constructs. Thus, when constructs cultured under free-swelling and dynamic loading were analyzed

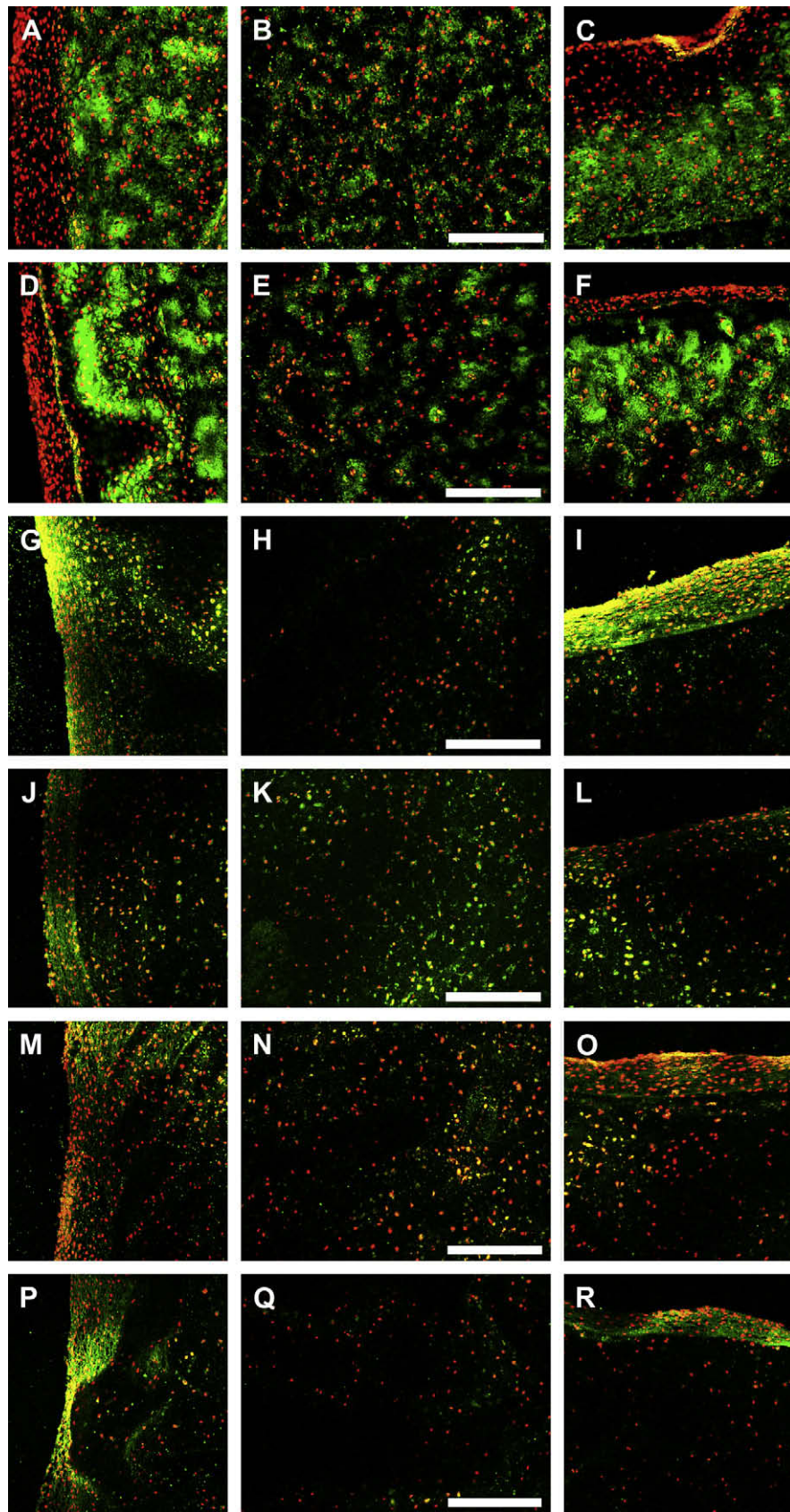


Fig. 7. Immunofluorescent labeling (green) for type II collagen (A–F), type I collagen (G–L), and elastin (M–R) of free-swelling (A–C, G–I, M–O) and dynamically loaded (D–F, J–L, P–R) chondrocyte-seeded constructs at day 42. Images were acquired along the radial edge (first column), in the center (second column), and along the axial edge (third column) of the constructs. Propidium iodide counter staining (red) was used to visualize the cell nuclei. Scale bars equal 200 μm .

separately, these correlations for whole constructs were maintained for the dynamically loaded group only. With coring the correlation between the GAG content and the moduli was maintained in the cores, but was lost in the annuli of the loaded constructs. Coring also reduced the correlation between the collagen content and the dynamic modulus of the annuli, however, a strong correlation between the collagen content and both moduli was still observed in the central core of dynamically loaded constructs. The disruption of the collagen network and of the fibrous capsule may explain the loss of correlation in collagen content and dynamic modulus in the annuli, which contained more of the fibrous tissue than the cores. Nevertheless, taken together, these results confirm our expectation that the changes in the equilibrium stiffness of the constructs over time may be due primarily to the elaborated GAG molecules. Additionally, these results indicate that the collagen content plays a more significant role in the dynamic stiffness of the dynamically loaded constructs than free-swelling controls, possibly indicating structural adaptation to mechanical stimuli. A more highly organized collagen fiber network, which we believe is generated by the radial tensile strain associated with dynamic unconfined compression loading^{2,29}, may contribute to the significantly stiffer dynamic modulus observed for the loaded constructs at day 42. This explanation is supported by polarized light images of radial fiber alignment in dynamically loaded constructs reported previously².

While mechanical properties and GAG content generally did not exhibit differences between the core and annular regions, other measures did show significant differences. The absolute DNA content of cores was lower than annuli on day 0, but this is likely due to differences in size as wet weight-normalized data shows no significant differences. The annuli, however, did increase in DNA content, in both absolute and wet weight-normalized data, compared to cores over time in culture. This increase in annuli DNA content may also be partially due to the heavily cellular outgrowth formed on the construct over time in culture. Less collagen per wet weight was produced in central core regions compared to their respective annular regions, which is consistent with our finding that the central region of constructs exhibited less intense staining for collagen compared to the outer edges (Figs. 6 and 7)². The most likely explanation for these observations is transport limitation for nutrients and waste products; whereas solute transport between the central core and the culture medium occurs primarily through the axial surfaces of the construct (top surface), the annular region also benefits from transport through the circumferential surface (radial edge). Transport limitations may be exacerbated by the formation of the dedifferentiated cell layer on the construct in terms of nutrient consumption and diffusion length. Dynamic loading, which is expected to enhance nutrient transport⁵, had an influence on GAG content in the cores and annuli, but not on collagen content, indicating a preferential mechanotransduction mechanism that warrants further investigation.

The findings of this study may be specific to our chondrocyte-seeded agarose hydrogel system and may not necessarily extend to more porous and permeable scaffolds. Seidel and co-workers reported that the material properties of chondrocyte-seeded polyglycolic acid (PGA) constructs did not benefit from culturing in a perfusion-mechanical stimulation bioreactor after a 30-day free-swelling culture period²⁵. In contrast to the current study, GAG levels with loading were observed to drop with culture time. In addition, GAG normalized by wet weight was generally similar for

central core regions and annular ring regions of constructs in our study, but was significantly decreased in the annular region for the PGA constructs. These results likely indicate that the effects of applied deformational loading are scaffold-dependent; indeed it is possible that the greater permeability of the PGA constructs would lead to greater amounts of GAG loss during loading.

In summary, this study shows that chondrocyte-seeded agarose disks do not exhibit significant inhomogeneity in material properties and GAG content along the radial direction, and collagen synthesis progresses at a slower rate in the core relative to the annular regions. The mechanical properties are governed predominantly by the GAG content, at least up to the stage of maturation achieved here. Dynamic loading enhanced the material properties and GAG content relative to free-swelling controls, but did not alter the spatial homogeneity. While nutrient transport limitations might explain the radial variation in DNA and collagen content, this does not appear to affect GAG distribution, most likely because chemical signals and building blocks for GAG synthesis remain available at sufficient levels in the center of the constructs. As this study represents the first attempts to characterize the radial development of engineered cartilage constructs, it is important to acknowledge the pitfalls of the adopted experimental design: it is possible that any effects of the fluid flow gradient produced during loading were masked by the coarseness of the coring technique used in the presented study. Future experiments may utilize smaller cores from various locations to better characterize the development of *de novo* matrix in the radial direction. In addition, the fibrous tissue formation and known variability of serum³⁰ motivate the adoption of serum-free media for future research.

Conflict of interest

There are no conflicts of interest or sources of bias in the research contained in this manuscript.

Acknowledgments

Funded by the NIH [AR46568 (CTH), AR49922 (CTH), graduate supplement (TNK)].

References

1. Mauck RL, Soltz MA, Wang CC, Wong DD, Chao PH, Valhmu WB, *et al.* Functional tissue engineering of articular cartilage through dynamic loading of chondrocyte-seeded agarose gels. *J Biomech Eng* 2000; 122:252–60.
2. Kelly TA, Ng KW, Wang CC, Ateshian GA, Hung CT. Spatial and temporal development of chondrocyte-seeded agarose constructs in free-swelling and dynamically loaded cultures. *J Biomech* 2005;39: 1489–97.
3. Ateshian GA, Wang H. A theoretical solution for the frictionless rolling contact of cylindrical biphasic articular cartilage layers. *J Biomech* 1995;28:1341–55.
4. Park S, Krishnan R, Nicoll SB, Ateshian GA. Cartilage interstitial fluid load support in unconfined compression. *J Biomech* 2003;36: 1785–96.
5. Mauck RL, Hung CT, Ateshian GA. Modeling of neutral solute transport in a dynamically loaded porous permeable gel: implications for articular cartilage biosynthesis and tissue engineering. *J Biomech Eng* 2003;125:602–14.
6. Mow VC, Wang CCB, Hung CT. The extracellular matrix, interstitial fluid and ions as a mechanical signal transducer in articular cartilage. *Osteoarthritis Cartilage* 1999;7:41–58.
7. Armstrong CG, Lai WM, Mow VC. An analysis of the unconfined compression of articular cartilage. *J Biomech Eng* 1984;106:165–73.

8. Armstrong CG, Mow VC. The mechanical properties of articular cartilage. *Bull Hosp Jt Dis Orthop Inst* 1983;43:109–17.
9. Quinn TM, Grodzinsky AJ, Buschmann MD, Kim YJ, Hunziker EB. Mechanical compression alters proteoglycan deposition and matrix deformation around individual cells in cartilage explants. *J Cell Sci* 1998;111(Pt 5):573–83.
10. Kim YJ, Sah RL, Grodzinsky AJ, Plaas AH, Sandy JD. Mechanical regulation of cartilage biosynthetic behavior: physical stimuli. *Arch Biochem Biophys* 1994;311:1–12.
11. Buschmann MD, Kim YJ, Wong M, Frank E, Hunziker EB, Grodzinsky AJ. Stimulation of aggrecan synthesis in cartilage explants by cyclic loading is localized to regions of high interstitial fluid flow. *Arch Biochem Biophys* 1999;366:1–7.
12. Soltz MA, Ateshian GA. Interstitial fluid pressurization during confined compression cyclical loading of articular cartilage. *Ann Biomed Eng* 2000;28:150–9.
13. Riesle J, Hollander AP, Langer R, Freed LE, Vunjak-Novakovic G. Collagen in tissue-engineered cartilage: types, structure, and crosslinks. *J Cell Biochem* 1998;71:313–27.
14. McGowan KB, Kurtis MS, Lottman LM, Watson D, Sah RL. Biochemical quantification of DNA in human articular and septal cartilage using PicoGreen and Hoechst 33258. *Osteoarthritis Cartilage* 2002;10:580–7.
15. Farndale RW, Buttle DJ, Barrett AJ. Improved quantitation and discrimination of sulphated glycosaminoglycans by use of dimethylmethylene blue. *Biochim Biophys Acta* 1986;883:173–7.
16. Stegemann H, Stalder K. Determination of hydroxyproline. *Clin Chim Acta* 1967;19:267–73.
17. Hollander AP, Heathfield TF, Webber C, Iwata Y, Bourne R, Rorabeck C, *et al.* Increased damage to type II collagen in osteoarthritic articular cartilage detected by a new immunoassay. *J Clin Invest* 1994;93:1722–32.
18. Lin W, Shuster S, Maibach HI, Stern R. Patterns of hyaluronan staining are modified by fixation techniques. *J Histochem Cytochem* 1997;45:1157–63.
19. Mow VC, Kuei SC, Lai WM, Armstrong CG. Biphasic creep and stress relaxation of articular cartilage in compression? Theory and experiments. *J Biomech Eng* 1980;102:73–84.
20. Kelly TA, Wang CC, Mauck RL, Ateshian GA, Hung CT. Role of cell-associated matrix in the development of free-swelling and dynamically loaded chondrocyte-seeded agarose gels. *Biorheology* 2004;41:223–37.
21. Mauck RL, Seyhan SL, Ateshian GA, Hung CT. Influence of seeding density and dynamic deformational loading on the developing structure/function relationships of chondrocyte-seeded agarose hydrogels. *Ann Biomed Eng* 2002;30:1046–56.
22. Mauck RL, Wang CC, Oswald ES, Ateshian GA, Hung CT. The role of cell seeding density and nutrient supply for articular cartilage tissue engineering with deformational loading. *Osteoarthritis Cartilage* 2003;11:879–90.
23. Ng KW, Mauck RL, Statman LY, Lin EY, Ateshian GA, Hung CT. Dynamic deformational loading results in selective application of mechanical stimulation in a layered, tissue-engineered cartilage construct. *Biorheology* 2006;43:497–507.
24. Kisiday JD, Kurz B, DiMicco MA, Grodzinsky AJ. Evaluation of medium supplemented with insulin–transferrin–selenium for culture of primary bovine calf chondrocytes in three-dimensional hydrogel scaffolds. *Tissue Eng* 2005;11:141–51.
25. Seidel JO, Pei M, Gray ML, Langer R, Freed LE, Vunjak-Novakovic G. Long-term culture of tissue engineered cartilage in a perfused chamber with mechanical stimulation. *Biorheology* 2004;41:445–58.
26. Naumann A, Dennis JE, Awadallah A, Carrino DA, Mansour JM, Kastenbauer E, *et al.* Immunochemical and mechanical characterization of cartilage subtypes in rabbit. *J Histochem Cytochem* 2002;50:1049–58.
27. Yeh AT, Hammer-Wilson MJ, Van Sickle DC, Benton HP, Zoumi A, Tromberg BJ, *et al.* Nonlinear optical microscopy of articular cartilage. *Osteoarthritis Cartilage* 2005;13:345–52.
28. Moretti M, Wendt D, Schaefer D, Jakob M, Hunziker EB, Heberer M, *et al.* Structural characterization and reliable biomechanical assessment of integrative cartilage repair. *J Biomech* 2005;38:1846–54.
29. Loba EG, Wren TA, Beaupre GS, Carter DR. Mechanobiology of soft skeletal tissue differentiation – a computational approach of a fiber-reinforced poroelastic model based on homogeneous and isotropic simplifications. *Biomech Model Mechanobiol* 2003;2:83–96.
30. Honn KV, Singley JA, Chavin W. Fetal bovine serum: a multivariate standard. *Proc Soc Exp Biol Med* 1975;149:344–7.